New Carbazole-Based Conjugated Polymers Containing Pyridylvinyl Thiophene Units for Polymer Solar Cell Applications: Morphological Stabilization Through Hydrogen Bonding

SO-LIN HSU, CHIA-MIN CHEN, YU-HSIN CHENG, KUNG-HWA WEI

Department of Materials Science and Engineering, National Chiao Tung University, Hsinchu 30010, Taiwan

ABSTRACT: We have synthesized two conjugated polymers (**P1**, **P2**) containing alternating electron-donating and -accepting units, based on *N*-alkyl-2,7-carbazole, 4,7-di(thiophen-5-yl)-2,1,3-benzothiadiazole and 3-[2-(4-pyridyl)vinyl]thiophene units. These conjugated polymers contained different contents of pyridine units, which were incorporated to form hydrogen bonds with [6,6]-phenyl-C_{61}-butyric acid (PCBA). When these hydrogen bonding interactions were present in the polymer thin films, their thermal stability improved; deterioration, which occurred through aggregation of PCBA methyl ester after lengthy annealing times, was also suppressed. The power conversion efficiency of a device incorporating the film featuring hydrogen bonding interactions remained at 75% of the original value after thermal annealing for 5 h at 140 °C. © 2010 Wiley Periodicals, Inc. J Polym Sci Part A: Polym Chem 49: 603–611, 2011

KEYWORDS: conjugated polymers; phase separation; photovoltaic cells; polycarbazole; polycondensation

INTRODUCTION Polymer solar cells (PSCs) have attracted much attention because they offer great potential to produce light-weight, flexible, inexpensive, large-area devices. Among the many, conjugated polymers have been developed for solar cell applications;[1–5] regioregular poly(3-hexylthiophene) (P3HT) remains one of the most suitable for PSCs.[6–14] The power conversion efficiency (PCE) of a bulk heterojunction (BHJ) PSC made from blends of P3HT and [6,6]-phenyl-C_{71}-butyric acid methyl ester ($PC_{71}BM$) is approximately 5%.[12–14] The efficiency of PSCs rises to over 6% when using recently developed low-band gap conjugated polymers;[15–18] the highest PCE reported to date (7.73%) was that for a PSC fabricated from a poly[4,8-bis-substituted-benzo[1,2-b:4,5-b′]dithiophene-2,6-diyl-*alt*-4-substituted-thieno[3,4-b]thiophene-2,6-diyl]/$PC_{71}BM$ blend.[19]

For a BHJ PSC, controlling the blend morphology at the microscopic scale is critical for optimizing its PCE.[20] Several methods have been developed to control the blend morphology, including thermal annealing and solvent annealing of blends,[7,20–22] slow drying of spin-casted films,[12,23–25] and addition of high-boiling point additives.[26,27] Although the best BHJ morphology in a solar cell is believed to be a bicontinuous composite of donor and acceptor components with phase segregation on a suitable length scale (20–30 nm),[3,28] this morphology is not stable toward annealing for long periods (>30 min) at high temperatures (>130 °C). During thermal annealing, the molecules of PCBM diffuse through the film to form microsized aggregates. This process, which is accelerated under the constant flux of thermal energy generated by solar irradiation, decreases the donor–acceptor interfacial area and thereby decreases the PCE.[29] To achieve durable PSCs, the nanometer-scale morphological features of the BHJ device must be preserved. Two strategies have been developed to obtain stable BHJ morphologies. In the first, a thermal or photocrosslinkable P3HT material is used in the BHJ solar cell,[30,31] stabilizing the BHJ morphology and partially suppressing the deterioration of the PSC's performance. The hole mobility of the crosslinked P3HT domain, however, also decreased, leading to lower values for the short-circuit current density (J_{sc}) and PCE. In the second approach, the fullerene derivatives are grafted onto the side chains of the P3HT backbone[32–34] to reduce the rate of degradation of the PSC performance, as evidenced through accelerated thermal testing. In those reported polymers, however, the fullerene grafting percentage was relatively low (1%); as a result, the morphological stabilization was limited.

Because our ability to control the morphology directly through covalent bonding is somewhat limited, an alternative approach toward achieving ideal morphologies is to take advantage of supramolecular noncovalent interactions, namely hydrogen bonding, π stacking, and Coulombic interactions. Huang et al.[35] reported photovoltaic devices built through hierarchical self-assembly using a self-assembled monolayer (capable of forming hydrogen bonds) on gold and a combination of a barbituric acid-appended fullerene and a complementary melamine-terminated π-conjugated thiophene-based oligomer.

The incorporation of these electron donor (oligomer) and acceptor (fullerene derivative) assemblies into simple photovoltaic devices as thin film led to a 2.5-fold enhancement in photocurrent relative to that of the analogous system lacking hydrogen bonding between the donor and acceptor units. The development of such self-assembly techniques remains a scientific and technological challenge; if overcome, however, it could lead to a breakthrough in the creation of new molecular devices. Following such an approach, in this study, we synthesized two conjugated polymers (**P1**, **P2**) containing alternating electron-donating and -accepting units based on *N*-alkyl-2,7-carbazole, 4,7-di(thiophen-5-yl)-2,1,3-benzothiadiazole and 3-[2-(4-pyridyl)vinyl]thiophene units. Both polymers were synthesized through Suzuki coupling of 2,7-bis(4,4,5,5-tetramethyl-1,3,2-dioxaborolane-2-yl)-*N*-9′-heptadecanylcarbazole with 4,7-(2′-dibromothien-5-yl)-2,1,3-benzothiadiazole and 2,5-dibromo-3-[2-(4-pyridyl)vinyl]thiophene. The conjugated polymers contained various amounts of 3-[2-(4-pyridyl)vinyl]thiophene units, which were capable of forming hydrogen bonds with [6,6]-phenyl-C_{61}-butyric acid (PCBA) units. We also investigated the effect of thermal annealing (140 °C) for long periods of time on the morphological stabilization of the corresponding BHJ films and on the device performance.

EXPERIMENTAL

Materials

PCBM was purchased from Nano-C. All solvents were purchased from Aldrich, J. T. Baker, or Tedia and used as received, except for tetrahydrofuran (THF), *N*,*N*-dimethylformamide, and toluene, which were purified prior to use. All other chemicals were purchased in reagent grade from Aldrich, Acros, TCI, or Lancaster Chemical and used as received.

Characterization

^{1}H and ^{13}C NMR spectra were recorded using a Varian Unity-300 spectrometer. The molecular weights of the polymers were measured using gel permeation chromatography, with a Waters 2414 differential refractometer and a Waters Styragel column (polystyrene standards, THF as the eluent). UV–Vis absorption spectra were recorded using an HP 8453 spectrophotometer. Photoluminescence spectra were recorded using a Hitachi F-4500 luminescence spectrometer. Thermogravimetric analysis (TGA) was performed under a N_2 atmosphere using a Du Pont TGA 2950 apparatus operated at a heating rate of 10 °C min^{-1}. Differential scanning calorimetry (DSC) was performed under a N_2 atmosphere using a PerkinElmer Pyris DSC1 instrument operated at a heating rate of 10 °C min^{-1}. Cyclic voltammetry (CV) was performed using a BAS 100 electrochemical analyzer and a conventional three-electrode cell: a carbon glass electrode coated with the polymer thin film as the working electrode, a Pt wire as the counter electrode, and Ag/Ag$^+$ (0.01 M AgNO$_3$) as the reference electrode. Tetrabutylammonium hexafluorophosphate (0.1 M) in acetonitrile was used as the electrolyte for the CV measurements; the curves were calibrated using ferrocene [the highest occupied molecular orbital (HOMO) of which is -4.8 eV with respect to zero vacuum level] as the standard. The topographies of the polymer/PCBM films were measured using atomic force microscopy (AFM); a Digital Instruments Nanoscope IIIa apparatus was operated in tapping mode under ambient conditions.

Synthetic Procedures

2,7-Bis(4,4,5,5-tetramethyl-1,3,2-dioxaborolane-2-yl)-*N*-9′-heptadecanylcarbazole and 4,7-di(2′-bromothien-5′-yl)-2,1,3-benzothiadiazole were prepared according to the reported procedures.[36] The monomer **M1**, PCBA, and the copolymers **P1** and **P2** were prepared as outlined in Scheme 1.

2,5-Dibromo-3-methylthiophene (1)

N-Bromosuccinimide (NBS, 38.1 g, 0.210 mol) was added to a solution of 3-methylthiophene (10.0 g, 0.110 mol) in THF (80 mL) and AcOH (80 mL) at room temperature. After stirring for 3 h, CHCl$_3$ was added and the resulting mixture washed three times with water. The organic layer was dried (MgSO$_4$) and concentrated under reduced pressure. The crude product was distilled at 90 °C under vacuum to yield **1** (22.6 g, 87%).

^{1}H NMR (300 MHz, CDCl$_3$, ppm): δ 6.74 (s, 1H), 2.12 (m, 3H). ^{13}C NMR (75 MHz, CDCl$_3$, ppm): δ 138.3, 132.1, 110.3, 108.6, 15.4. Anal. Calcd: C, 23.46; H, 1.58. Found: C, 23.42; H, 1.60.

2,5-Dibromo-3-(bromomethyl)thiophene (2)

NBS (8.90 g, 50.0 mmol) and benzoyl peroxide (10 mg, 0.04 mmol) were added to a solution of **1** (12.8 g, 50.0 mmol) in CCl$_4$ (100 mL), which was then heated under reflux for 6 h. After cooling to room temperature, the mixture was washed sequentially with water ($2\times$ 300 mL), saturated NaHCO$_3$ ($1\times$ 300 mL), and water again ($1\times$ 300 mL). The organic phase was dried (MgSO$_4$) and concentrated under reduced pressure. The crude product was distilled at 105 °C under vacuum to yield **2** (14.1 g, 84%).

^{1}H NMR (300 MHz, CDCl$_3$, ppm): δ 6.97 (s, 1H), 4.34 (m, 2H). Anal. Calcd: C, 17.93; H, 0.90. Found: C, 16.53; H, 1.00.

4-[2-(2,5-Dibromothiophen-3-yl)vinyl]pyridine (M1)

A mixture of **2** (10.0 g, 30.0 mmol) and triethyl phosphite (4.98 g, 30.0 mmol) was heated at 160 °C for 3 h. After cooling to room temperature, the triethyl phosphite was distilled off at 120 °C. The residue was dissolved in dry THF (20 mL) and cooled in an ice-water bath (0 °C). A solution of NaOMe (1.80 g, 33.3 mmol) in dry THF (10 mL) was added portionwise to the mixture, which was then stirred for 10 min. A solution of 4-pyridinecarboxaldehyde (3.21 g, 30.0 mmol) in dry THF was added via syringe to the mixture, which was then stirred at room temperature for 12 h before being poured into water and extracted with diethyl ether. The combined organic phases were washed three times with water and then dried (MgSO$_4$). After evaporating the solvent under reduced pressure, the crude product was purified through chromatography (SiO$_2$; EtOAc/hexane, 1:5). Recrystallization (MeOH/hexane) afforded **M1** as a white solid (6.91 g, 67%).
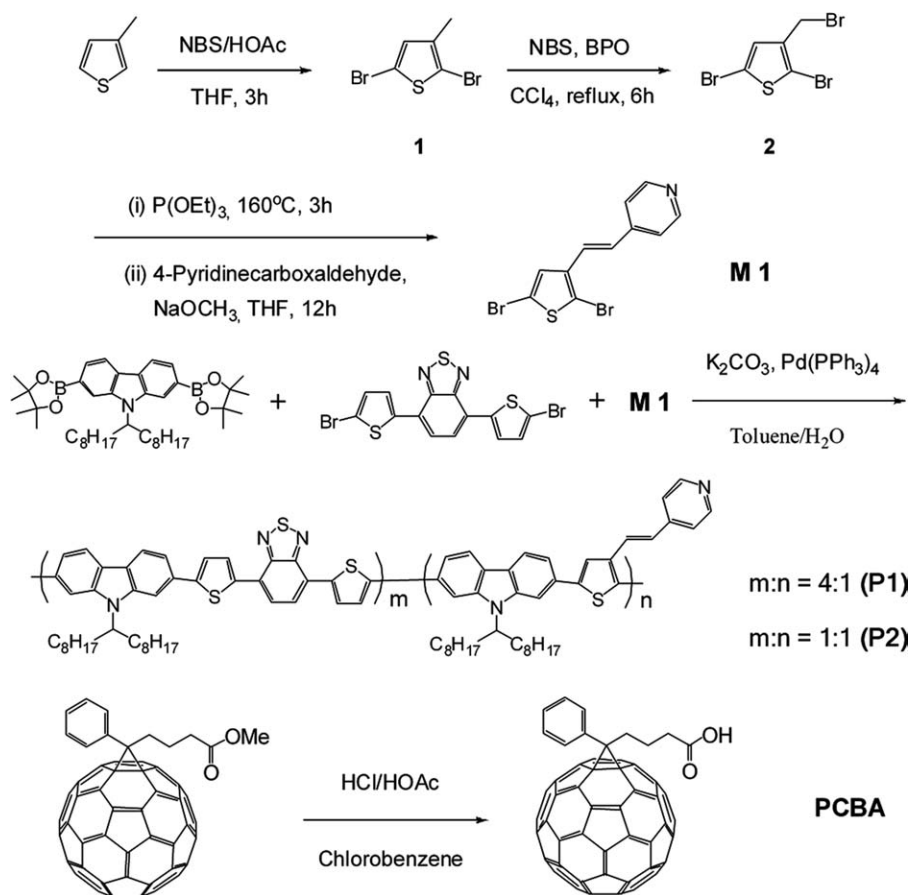
SCHEME 1 Synthesis of monomers, the copolymers **P1** and **P2**, and PCBA.

^{1}H NMR (300 MHz, CDCl$_3$, ppm): δ 8.58 (d, J = 1.5 Hz, 1H), 8.56 (d, J = 1.5 Hz, 1H), 7.34 (d, J = 1.8 Hz, 1H), 7.32 (d, J = 1.8 Hz, 1H), 7.21 (s, 1H), 7.14 (d, J = 16.2 Hz, 1H), 6.82 (d, J = 16.2 Hz, 1H). ^{13}C NMR (75 MHz, CDCl$_3$, ppm): δ 150.6, 144.1, 138.4, 128.7, 127.6, 124.4, 123.0, 121.1, 112.7. Anal. Calcd: C, 38.29; H, 2.04; N, 4.06. Found: C, 38.73; H, 2.49; N, 3.99.

P1 (m:n = 4:1)

Pd(PPh$_3$)$_4$ (7 mg, 0.006 mmol) was added to a degassed mixture of **M1** (21.0 mg, 0.0600 mmol), 2,7-bis(4,4,5,5-tetra-methyl-1,3,2-dioxaborolane-2-yl)-N-9'-heptadecanylcarbazole (200 mg, 0.30 mmol), 4,7-di(2'-bromothien-5'-yl)-2,1,3-ben-zothiadiazole (111.4 mg, 0.240 mmol), K$_2$CO$_3$ (276.4 mg, 2.00 mmol), H$_2$O (1 mL), Aliquat 336 (36 mg), and toluene (5 mL) at 60 °C and then the mixture was stirred and heated under reflux for 4 h under a N$_2$ atmosphere. At this point, phenylboronic acid (37 mg, 0.03 mmol) was added and the mixture was heated under reflux for a further 1 h; bromo-benzene (0.03 mL, 0.03 mmol) was then added and the mixture was heated under reflux for another 1 h. The reaction mixture was poured into MeOH (100 mL) and the resulting black precipitate was collected through filtration. The precipitated polymer was washed with MeOH, acetone, and hex-ane in a Soxhlet apparatus for 24 h to remove any oligomers and catalyst residues, thereby providing **P1** (172 mg, 83%).

^{1}H NMR (300 MHz, CDCl$_3$, ppm): δ 8.50 (s, 2H), 8.17–8.11 (m, 15H), 7.97–7.41 (m, 34H), 7.19 (s, 1H), 7.17 (s, 8H), 6.89 (s, 1H), 4.66 (br, 5H), 2.39 (br, 10H), 1.98 (br, 10H), 1.23–1.13 (br, 120H), 0.76 (s, 30H). Anal. Calcd: C, 74.94; H, 7.02; N, 5.77. Found: C, 72.65; H, 6.90; N, 5.68.

P2 (m:n = 1:1)

Using the same procedure described above for **P1**, the reac-tion of **M1** (52.5 mg, 0.150 mmol), 2,7-bis(4,4,5,5-tetra-methyl-1,3,2-dioxaborolane-2-yl)-N-9'-heptadecanylcarbazole (200 mg, 0.300 mmol), 4,7-di(2'-bromothien-5'-yl)-2,1,3-ben-zothiadiazole (69.6 mg, 0.150 mmol), K$_2$CO$_3$ (276.4 mg, 2.00 mmol), H$_2$O (1 mL), Aliquat 336 (36 mg), toluene (5 mL), and Pd(PPh$_3$)$_4$ (7 mg, 0.006 mmol) afforded **P2** as a black solid (151 mg, 77%).

^{1}H NMR (300 MHz, CDCl$_3$, ppm): δ 8.53 (s, 2H), 8.20–8.11 (m, 6H), 7.97–7.43 (m, 13H), 7.19 (s, 1H), 7.11 (s, 2H), 6.90 (s, 1H), 4.70 (br, 2H), 2.39 (br, 4H), 2.02 (br, 4H), 1.25–1.16 (br, 48H), 0.79 (s, 12H). Anal. Calcd: C, 77.21; H, 7.43; N, 5.43. Found: C, 75.37; H, 7.46; N, 5.14.

PCBA

AcOH (3.8 mL) and conc. HCl (1.5 mL) were added at room temperature to a solution of PCBM (50.0 mg, 0.05 mmol) in chlorobenzene (6 mL) and then the mixture was stirred for 10 min before being heated at 110 °C for 12 h. After cooling, the reaction mixture was poured into MeOH (100 mL) and the precipitate was purified through repeated (three times) precipitation from CS$_2$ solution into MeOH (172 mg, 83%).

TABLE 1 Molecular Weights and Thermal Properties of the Copolymers

Polymer	M_n (g mol^{-1})	M_w (g mol^{-1})	PDI	T_d (°C)	T_g (°C)
P1	88,031	148,954	1.69	344	129
P2	26,357	129,517	4.91	393	148

^{1}H NMR (300 MHz, CDCl$_3$/CS$_2$, ppm): δ 9.58 (s, 1H), 7.91 (s, 2H), 7.54–7.45 (m, 3H), 2.94 (s, 2H), 2.54 (s, 2H), 2.18 (s, 2H). Anal. Calcd: C, 95.08; H, 1.35. Found: C, 95.02; H, 1.37.

Photovoltaic Device Fabrication

The current density–voltage (*J*–*V*) properties of the polymers were determined for devices having the sandwich structure [indium tin oxide (ITO)/poly(3,4-ethylenedioythiophene): poly(styrene sulfonic acid) (PEDOT:PSS)/polymer:PCBM/Ca/Al]. First, an ITO-coated glass substrate was etched with acid and cleaned sequentially using detergent, deionized water, acetone, and isopropyl alcohol. The cleaned substrate was treated with ozone plasma for 5 min and then a 30 nm layer of PEDOT (Batron P AL 4083, HC Stark) was spin coated onto it. The PEDOT-coated substrate was heated at 150 °C for 30 min to ensure that all of the solvents had been removed. The active layer of the device was spin coated at 1200 rpm from a 1,2-dichlorobenzene solution containing the polymer and PCBM (1:2, w/w). The thickness of the polymer/PCBM layer was about 100 nm. After thermal annealing of the active layer (140 °C, 10 min), a layer of Ca (35 nm) was vapor deposited as the cathode and a layer of Al (100 nm) as the protecting layer under a base pressure of less than 1×10^{-6} Torr. The effective area of an accomplished device was 0.04 cm^2. The sample devices were tested under simulated AM 1.5G illumination (100 mW cm^{-2}) using a Xe lamp-based Newport 66902 150W solar simulator equipped with an AM1.5 filter as the white light source. An OPHIR thermopile 71964 was used to determine that the optical power at the sample was 100 mW cm^{-2}. The *J*–*V* characteristics of the samples were measured under a N$_2$ atmosphere using a Keithley 236 source-measurement meter. The external quantum efficiencies (EQEs) were measured using a Keithley 236 source-measure unit coupled with an Oriel Cornerstone 130 monochromator; the light intensity at each wavelength was calibrated using an OPHIR 71580 diode.

RESULTS AND DISCUSSION

Synthesis and Characterization

Scheme 1 displays the chemical structures and the synthetic route for preparing the copolymers **P1** and **P2** and PCBA. We synthesized the monomer **M1** through a Horner–Emmons reaction to form the conjugated pyridine–vinylene-substituted thiophene. The ^{1}H NMR spectrum of the monomer **M1** featured two sets of doublets (7.19–6.77 ppm) representing the two olefinic protons in the vinyl unit. The coupling constant of these two doublets (16.2 Hz) indicates that the main product of the reaction was the *trans* isomer. We polymerized 2,7-bis(4,4,5,5-tetramethyl-1,3,2-dioxaborolane-2-yl)-*N*-9′-heptadecanylcarbazole, 4,7-di(2′-bromothien-5′-yl)-

2,1,3-benzothiadiazole, and **M1** through Suzuki cross-coupling polycondensation to afford the copolymers **P1** and **P2** containing different mole percentages (10% and 25%, respectively) of pyridine side chains. According to size exclusion chromatography experiments (using monodisperse polystyrene standards and THF as the solvent), the number-average molecular weights of **P1** and **P2** were 88,031 and 26,357 g mol^{-1}, respectively, with corresponding polydispersity indices (PDIs) of 1.69 and 4.91, respectively (Table 1). We suspect that the molecular weight of **P2** was less than that of **P1** because the greater number of pyridylvinyl thiophene units disturbed the reactivity of the polycondensation. The copolymers **P1** and **P2** exhibited good solubility in 1,2-dichlorobenzene, CHCl$_3$, and THF; therefore, uniform thin films of the polymers were readily produced through spin coating for further study of PSC devices.

We synthesized PCBA through hydrolysis of its corresponding ester (PCBM) with HCl/AcOH (Scheme 1). The solubility of PCBA is good in CS$_2$, but it could also be dissolved sparingly in 1,2-dichlorobenzene, CHCl$_3$, and THF for further study. Figure 1 presents FTIR spectra of **P1**, PCBA, and a **P1**/PCBA blend. For polymer **P1**, characteristic C=C and C=N ring stretching of pyridine rings appeared in the range 1430–1600 cm^{-1}. When **P1** was mixed with PCBA, a broad peak appeared at 3100–3500 cm^{-1}, consistent with the formation of hydrogen bonds between the pyridine units on the polymer side chains and the carboxylic acid groups of PCBA units.

Thermal Properties

Table 1 summarizes the thermal properties of **P1** and **P2**, determined through DSC and TGA analyses performed under a N$_2$ atmosphere. TGA indicated that both polymers exhibited good thermal stability, with 5% decomposition temperatures (T_d) of 344 and 393 °C; the glass transition temperatures were 129 and 148 °C, respectively. This good thermal stability, which we ascribe to the presence of stiff carbazole
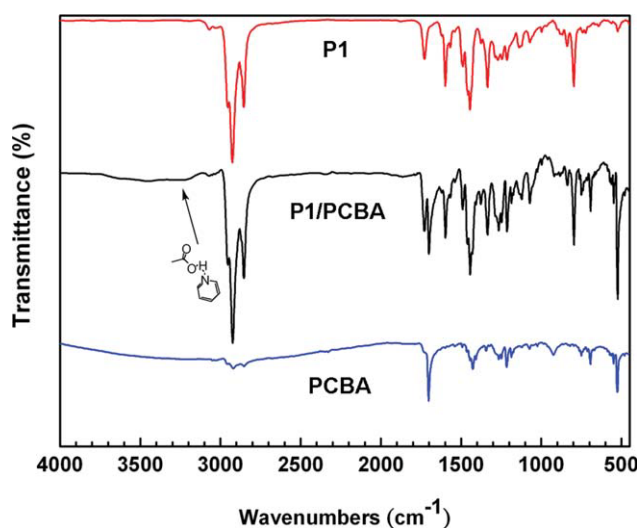

FIGURE 1 FTIR spectra of the copolymer **P1**, PCBA, and a **P1**/PCBA blend. [Color figure can be viewed in the online issue, which is available at wileyonlinelibrary.com.]
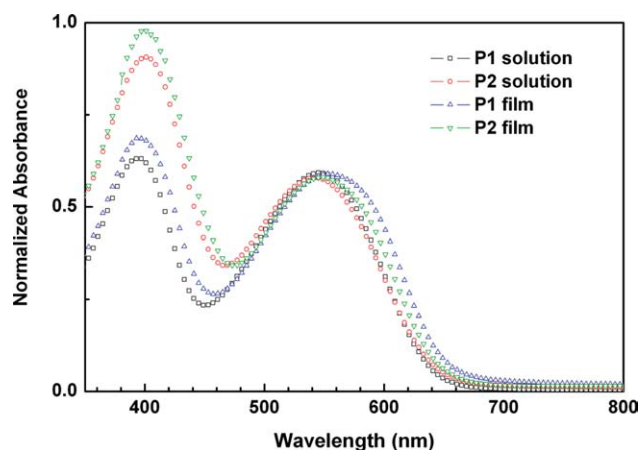
FIGURE 2 UV–Vis absorption spectra of the copolymers **P1** and **P2**. [Color figure can be viewed in the online issue, which is available at wileyonlinelibrary.com.]

units on the main chains, is also an important property for PSC devices to ensure resistance against deformation or degradation of the active layer.

Optical Properties

Figure 2 displays the absorption spectra of the two copolymers, measured both from dilute THF solutions and from thin films; Table 2 summarizes the correlated optical parameters. Both polymers exhibited two characteristic bands in their absorption spectra; the first, at about 395 nm, represents π–π^* transitions of the conjugated side chains, whereas the second, at longer wavelength, represents intramolecular charge transfer from the carbazole groups to the benzothiadiazole moieties in the conjugated main chains. The signal for the π–π^* transitions of **P2** (ca. 395 nm) has greater intensity and is slightly red shifted relative to that of **P1** (ca. 519 nm), due to the higher content of incorporated pyridylvinyl conjugated side chain on the polymer backbone of **P2**. Notably, the two characteristic bands in the absorption spectra (ca. 395, 550 nm) changed only slightly (by ca. 5 nm) after transfer from solution to the solid state, suggesting that only weak packing forces exist between the polymer chains, possibly due to steric hindrance resulting from the tethered pyridylvinyl units. The optical band gaps (E_g^{opt}), calculated from absorption onsets in the films, were 1.87 eV for **P1** and 1.91 eV for **P2**.

Electrochemical Properties

We used CV to estimate the HOMO and lowest unoccupied molecular orbital (LUMO) energy levels of the conjugated polymers (Table 2). Using ferrocene as the internal standard,

we calculated HOMO energy levels of **P1** and **P2** as -5.50 and -5.66 eV, respectively; these similar values are also close to the HOMO energy level of PCDTBT (-5.5 eV), presumably because of the similar main chain structures of these polymers.[36] The LUMO energy levels (ca. -3.6 eV for **P1**; -3.58 eV for **P2**) were located 0.2–0.3 eV above the LUMO energy level of the PCBM acceptor (-3.8 eV), thereby suggesting the possibility of energetically favorable electron transfer.

Photovoltaic Properties

To study the photovoltaic properties of these two polymers, we fabricated BHJ PSC devices having the structure ITO/PEDOT:PSS/polymer:PCBM/Ca/Al. The polymer (donor)/PCBM (acceptor) blend active layers were spin coated from 1,2-dichlorobenzene solutions at a concentration of 7 mg mL^{-1}. The photovoltaic properties of **P1** and **P2** were investigated initially using a 1:2 blending ratio, which was found to be optimal for the corresponding poly[N-9'-heptadecanyl-2,7-carbazole-alt-5,5-(4',7'-di-2-thienyl-2',1',3'-benzothiadiazole)] (PCDTBT) system.[17] For the system based on the **P1**/PCBM blend, we calculated a PCE of 1.05%, with a value of V_{oc} of 0.58 V, a value of J_{sc} of 4.89 mA cm^{-2}, and a fill factor (FF) of 0.37. For the device based on the **P2**/PCBM blend, the PCE was 0.36%, with values of V_{oc}, J_{sc}, and FF of 0.38 V, 2.56 mA cm^{-2}, and 0.34, respectively. The performance of the device based on **P2**/PCBM was considerably lower than that based on **P1**/PCBM, presumably because the increasing quantity of pyridylvinyl side-chain units accompanied with decreasing content of benzothiadiazole might significantly reduce the charge transfer ability in the polymer chain and alter the intermolecular interactions. It might also be attributed to the fact that **P2** had a lower molecular weight and poorer PDI value than that of **P1**. Therefore, we used **P1** in our subsequent studies of the photovoltaic properties of this system. Next, we introduced PCBA to observe the effects of hydrogen bond formation between the tethered pyridine units of the polymer and the carboxylic acid groups of PCBA units. The weight ratio of **P1** to PCBM to PCBA in the blend is 3:5:1. In this case, the molar ratio of pyridylvinyl side chain in **P1** to carboxylic acid in PCBA is equal to 1:1 because each pyridylvinyl group has only one active position to form a hydrogen bond with a carboxylic acid. The active layer was annealed at 140 °C for 10 min prior to deposition of Ca/Al cathode. The device based on this blend exhibited a PCE of 1.12%, with a value of V_{oc} of 0.58 V, a value of J_{sc} of 4.97 mA cm^{-2}, and a FF of 0.39 (the J–V characteristics are presented in Fig. 3). This device performed slightly better (J_{sc} = 4.97 mA cm^{-2}; FF = 0.39) than that based simply on a corresponding **P1**/PCBM

TABLE 2 Optical and Electrochemical Properties of the Copolymers

Polymer	λ_{max}, solution (nm)	λ_{max}, film (nm)	E_g^{opt} (eV)[a]	E_g^{EC} (eV)	E_{HOMO} (eV)	E_{LUMO} (eV)
P1	395, 545	395, 553	1.87	1.90	-5.50	-3.60
P2	401, 542	403, 549	1.91	2.08	-5.66	-3.58

[a] Calculated from the absorption onset in the absorption spectrum of the film.
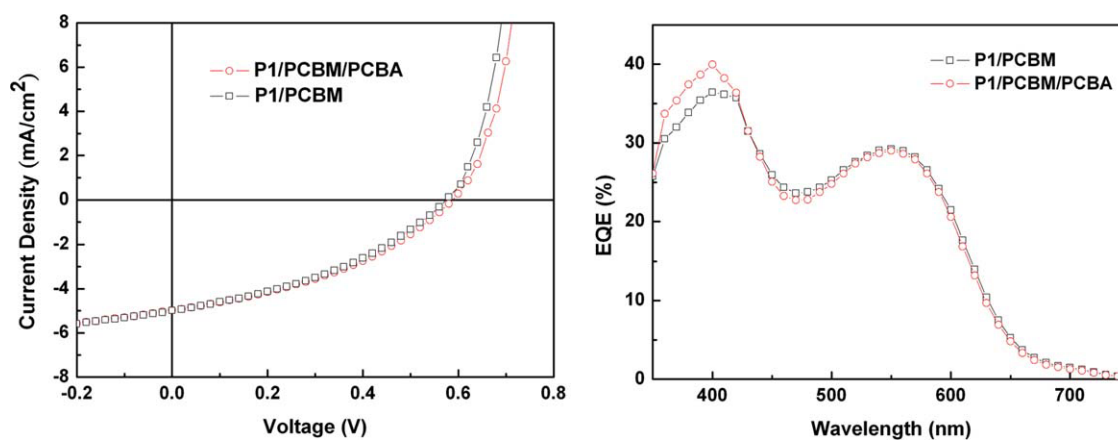
FIGURE 3 *J–V* characteristics and EQE spectra of devices based on **P1**/PCBM and **P1**/PCBM/PCBA blends. [Color figure can be viewed in the online issue, which is available at wileyonlinelibrary.com.]

blend (4.89 mA cm^{-2} and 0.37, respectively). EQE spectra of devices based on **P1**/PCBM and **P1**/PCBM/PCBA blends were also illustrated (Fig. 3). The PSC device based on the **P1**/PCBM/PCBA blend exhibited higher efficiency in its absorption in the UV region relative to that of the device based on **P1**/PCBM, presumably because π–π^* transitions were induced by the formation of hydrogen bonds in the polymer side chain, thereby increasing the photocurrent of the device.

Moreover, the curves display great coherence with their correlative absorptions of the active layers. These results suggest that incorporation of PCBA into the blending system dose not affect the charge transporting properties and film morphology. Finally, to verify the additional stability provided by hydrogen bonding interactions, we measured the device performances after various annealing times. Figure 4 reveals decreases in the PCEs of both devices over time; the rate of degradation of
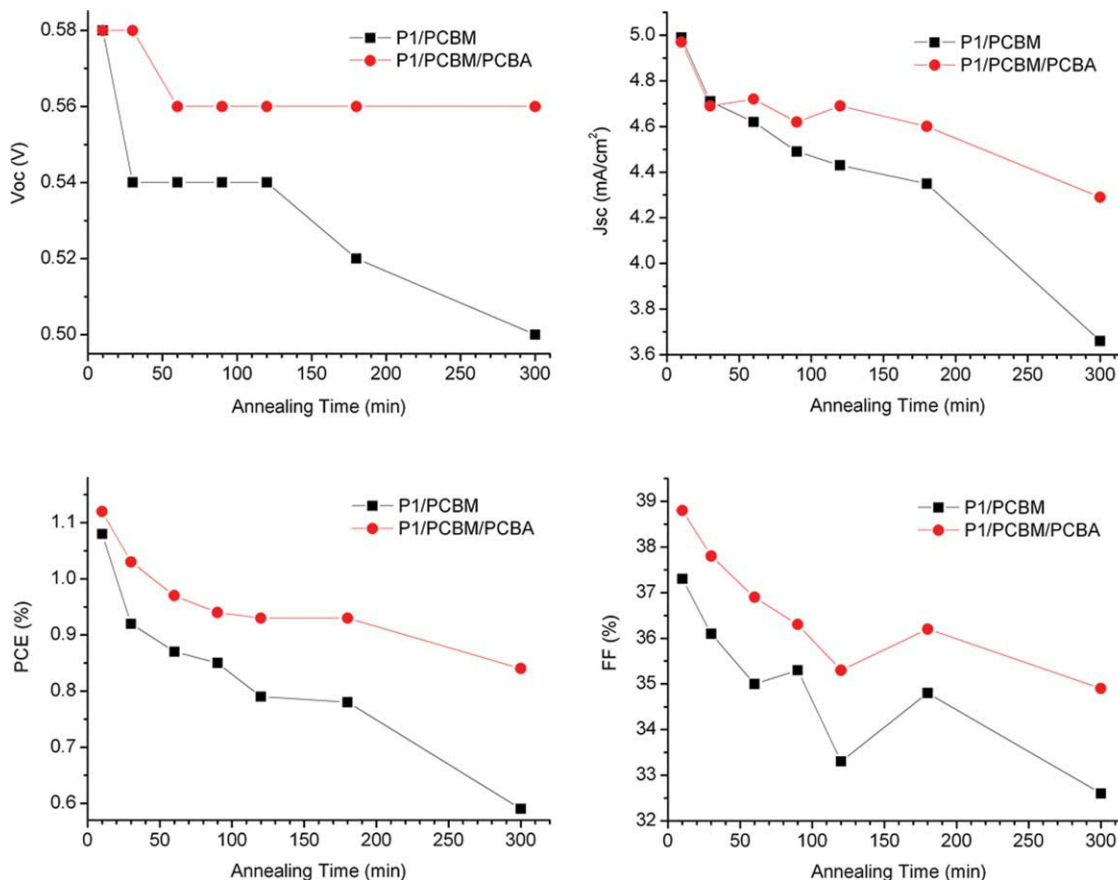

FIGURE 4 Devices performance plotted with respect to the annealing time at 140 °C for the **P1**/PCBM and **P1**/PCBM/PCBA blends. [Color figure can be viewed in the online issue, which is available at wileyonlinelibrary.com.]
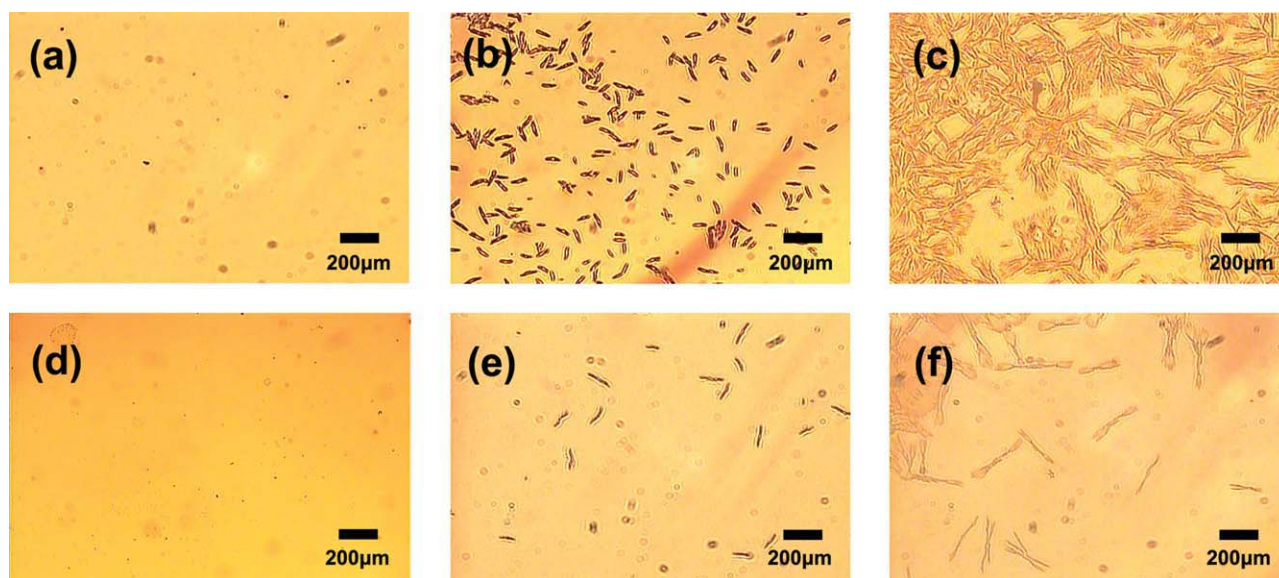
FIGURE 5 Optical micrographs of (a–c) **P1**/PCBM and (d–f) **P1**/PCBM/PCBA blend films that had been subjected to annealing at 140 °C for (a,d) 10 min, (b,e) 5 h, and (c,f) 10 h.

the **P1**/PCBM/PCBA film was, however, slower (decreasing by only 25% after thermal annealing for 5 h) than that of the **P1**/PCBM film (ca. 50% decrease). We ascribe this behavior to partial stabilization of the morphology of the active layer as a result of hydrogen bonding between the pyridine functional groups of the polymer and the carboxylic acid groups of the PCBA units; thus, while assembling with the polymer, PCBA simultaneously attracts its analog, PCBM, to form partial aggregates, thereby improving the degree of phase separation and increasing the interfacial area between the donor and acceptor units in the BHJ thin film.

Because the morphology of the active layer blends in the devices plays an important role in determining the device performance, we used optical microscopy to observe the morphological alteration on the micrometer scale. Figure 5 displays the morphological evolution within the thin films spin coated from **P1**/PCBM and **P1**/PCBM/PCBA blends after various annealing times. It is clear to find that thermal annealing induced the formation of needle-like crystals of PCBM molecules (length: hundreds of micrometers) in the **P1**/PCBM film; this phenomenon was greatly suppressed in the case of the **P1**/PCBM/PCBA blend. Thus, the assembled
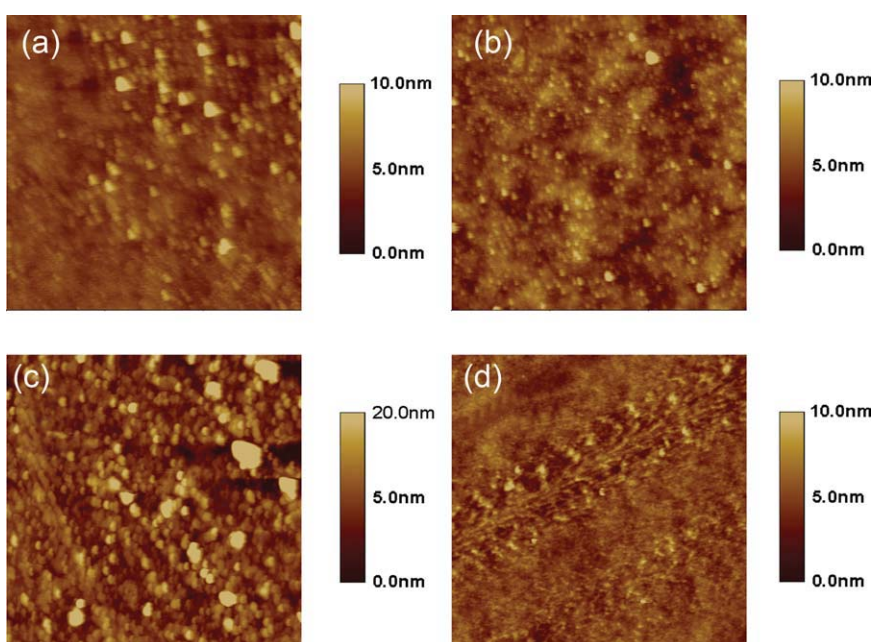

FIGURE 6 Topographic AFM images of the films based on (a,c) **P1**/PCBM and (b,d) **P1**/PCBM/PCBA blends; that had been subjected to annealing at 140 °C for (a,b) 10 min, (c,d) 5 h. Scale: 3×3 μm^2. [Color figure can be viewed in the online issue, which is available at wileyonlinelibrary.com.]

PCBA units successfully inhibited the large-scale aggregation of diffused PCBM molecules over time, thereby enhancing the morphological stabilization relative to that of the system lacking hydrogen bonding interactions.

To study of the morphological issues on the nanoscale, we monitored the topographies of the blend films using tapping-mode AFM. Figure 6 reveals that the **P1**/PCBM/PCBA and **P1**/PCBM films gave root-mean-square roughnesses of 0.65 and 1.07 nm after annealing for 10 min, respectively. However, after annealing for 5 h, the **P1**/PCBM/PCBA blend had a more uniform surface than that of the **P1**/PCBM blend, with root-mean-square roughnesses of 1.06 and 4.80 nm, respectively. Thus, it appears that the presence of an appropriate quantity of PCBA in the polymer blend prevented the PCBM units from undergoing severe aggregation during long-term annealing, possibly because the PCBM units were well dispersed through attraction to the PCBA units in each active site for hydrogen bonding. In summary, decreased surface roughness when hydrogen bonding was present, on both the micrometer and nanoscale scales, improved the photovoltaic performance of the PSC devices.

CONCLUSIONS

We have synthesized two polymers, **P1** and **P2**, through Suzuki couplings of 2,7-bis(4,4,5,5-tetramethyl-1,3,2-dioxaborolane-2-yl)-N-9'-heptadecanylcarbazole with 4,7-(2'-dibromothien-5-yl)-2,1,3-benzothiadiazole and 2,5-dibromo-3-[2-(4-pyridyl)vinyl]thiophene. Both polymers exhibited relatively high glass transition temperatures (129 and 148 °C, respectively). Although the photovoltaic properties decreased when we increased the content of side chain-tethered pyridine units from 10% to 25% (possibly because **P2** had a lower molecular weight and poorer PDI than did **P1**), the thermal stability improved after incorporating PCBA into **P1**, thereby forming hydrogen bonds in the polymer blend; the PCE of the PSC device based on **P1**/PCBM/PCBA remained at 75% of its original value after annealing for 5 h at 140 °C, but that based on **P1**/PCBM plunged to less than 55% of the original value under the same conditions. The morphological deterioration of the BHJ film of the **P1**/PCBM/PCBA blend was also suppressed, as observed through optical and AFM imaging.

REFERENCES AND NOTES

1 Winder, C.; Sariciftci, N. S. J Mater Chem 2004, 14, 1077–1086.

2 Bundgaard, E.; Krebs, F. C. Sol Energy Mater Sol Cells 2007, 91, 954–985.

3 Mayer, A. C.; Scully, S. R.; Hardin, B. E.; Rowell, M. W.; McGehee, M. D. Mater Today 2007, 10, 28–33.

4 Thompson, B. C.; Fréchet, J. M. J. Angew Chem Int Ed 2008, 47, 58–77.

5 Cheng, Y. J.; Yang, S. H.; Hsu, C. S. Chem Rev 2009, 109, 5868–5923.

6 Günes, S.; Neugebauer, H.; Sariciftci, N. S. Chem Rev 2007, 107, 1324–1338.

7 Hoppe, H.; Sariciftci, N. S. J Mater Chem 2006, 16, 45–61.

8 Thompson, B. C.; Fréchet, J. M. J. Angew Chem Int Ed 2008, 47, 58–77.

9 Chang, Y.-T.; Hsu, S.-L.; Su, M.-H.; Wei, K.-H. Adv Funct Mater 2007, 17, 3326–3331.

10 Chang, Y.-T.; Hsu, S.-L.; Chen, G.-Y.; Su, M.-H.; Singh, T. A.; Diau, E. W.-G.; Wei, K.-H. Adv Funct Mater 2008, 18, 2356–2365.

11 Chang, Y.-T.; Hsu, S.-L.; Su, M.-H.; Wei, K.-H. Adv Mater 2009, 21, 2093–2097.

12 Li, G.; Shrotriya, V.; Huang, J. S.; Yao, Y.; Moriarty, T.; Emery, K.; Yang, Y. Nat Mater 2005, 4, 864–868.

13 Ma, W. L.; Yang, C. Y.; Gong, X.; Lee, K. H.; Heeger, A. J. Adv Funct Mater 2005, 15, 1617–1622.

14 Yip, H.-L.; Hau, S. K.; Baek, N. S.; Ma, H.; Jen, A. K.-Y. Adv Mater 2008, 20, 2376–2382.

15 Hau, S. K.; Yip, H.-L.; Ma, H.; Jen, A. K.-Y. Appl Phys Lett 2008, 93, 233304-1–233304-3.

16 Blouin, N.; Michaud, A.; Gendron, D.; Wakim, S.; Blair, E.; Neagu-Plesu, R.; Belletête, M.; Durocher, G.; Tao, Y.; Leclerc, M. J Am Chem Soc 2008, 130, 732–742.

17 Wakim, S.; Beaupré, S.; Blouin, N.; Aich, B.-R.; Rodman, S.; Gaudiana, R.; Tao, Y.; Leclerc, M. J Mater Chem 2009, 19, 5351–5358.

18 Chu, T. Y.; Alem, S.; Verly, P. G.; Wakim, S.; Lu, J.; Tao, Y.; Beaupré, S.; Leclerc, M.; Bélanger, F.; Désilets, D.; Rodman, S.; Waller, D.; Gaudiana, R. Appl Phys Lett 2009, 95, 063304-1–063304-3.

19 Chen, H. Y.; Hou, J. H.; Zhang, S. Q.; Liang, Y. Y.; Yang, G. W.; Yang Y.; Yu, L. P.; Wu, Y.; Li, G. Nat Photonics 2009, 3, 649–653.

20 Campoy-Quiles, M.; Ferenczi, T.; Agostinelli, T.; Etchegoin, P. G.; Kim, Y. K.; Anthopoulos, T. D.; Stavrinou, P. N.; Bradley, D. D. C.; Nelson J. Nat Mater 2008, 7, 158–164.

21 Al-Ibrahim, M.; Ambacher, O.; Sensfuss, S.; Gobsch, G. Appl Phys Lett 2005, 86, 201120-1–201120-3.

22 Chirvase, D.; Parisi, J.; Hummelen, J. C.; Dyakonov, V. Nanotechnology 2004, 15, 1317–1323.

23 Zhao, Y.; Xie, Z.; Qu, Y.; Geng, Y.; Wang, L. Appl Phys Lett 2007, 90, 043504-1–043504-3.

24 Vanlaeke, P.; Vanhoyland, G.; Aernouts, T.; Cheyns, D.; Deibel, C.; Manca, J.; Heremans, P.; Poortmans, J. Thin Solid Films 2006, 511–512, 358–361.

25 Mihailetchi, V. D.; Xie, H.; de Boer, B.; Popescu, L. M.; Hummelen, J. C.; Blom, P. W. M.; Koster, L. J. A. Appl Phys Lett 2006, 89, 012107-1–012107-3.

26 Peet, J.; Senatore, M. L.; Heeger, A. J.; Bazan, G. C. Adv Mater 2009, 21, 1521–1527.

27 Coffin, R. C.; Peet, J.; Rogers, J; Bazan, G. C. Nat Chem 2009, 1, 657–661.

28 Ma, W.; Gopinathan, A.; Heeger, A. J. Adv Mater 2007, 19, 3656–3659.

29 Woo, C. H.; Thompson, B. C.; Kim, B. J.; Toney M. F.; Fréchet, J. M. J. J Am Chem Soc 2008, 130, 16324–16329.

30 Miyanishi, S.; Tajima, K.; Hashimoto, K. Macromolecules 2009, 42, 1610–1618.

31 Kim, B. J.; Miyamoto, Y.; Ma, B.; Fréchet, J. M. J. Adv Funct Mater 2009, 19, 2273–2281.

32 Chen, X.; Gholamkhass, B.; Han, X.; Vamvounis, G.; Hold-croft, S. Macromol Rapid Commun 2007, 28, 1792–1797.

33 Gholamkhass, B.; Peckham, T. J.; Holdcroft, S. Polym Chem 2010, 1, 708–719.

34 Gholamkhass, B.; Holdcroft, S. Chem Mater 2010, 22, 5371–5376.

35 Huang, C. H.; McClenaghan, N. D.; Kuhn, A.; Bravic, G.; Bassani, D. M. Tetrahedron 2006, 62, 2050–2059.

36 Blouin, N.; Michaud, A.; Leclerc, M. Adv Mater 2007, 19, 2295–2300.